

Single-photon device requirements for operating linear optics quantum computing outside the post-selection basis

Thomas Jennewein^{a,b,c*}, Marco Barbieri^{b,d} and Andrew G. White^b

^aInstitute for Quantum Computing, University of Waterloo, Waterloo, ON, Canada; ^bDepartment of Physics, and Centre for Quantum Computer Technology, University of Queensland, 4027 St Lucia, QLD, Australia; ^cInstitute for Quantum Information and Quantum Optics, Austrian Academy of Sciences, Vienna, Austria; ^dLaboratoire Charles Fabry, Institut d'Optique, 91127 Palaiseau, France

(Received 2 June 2010; final version received 29 November 2010)

Photonics is a promising architecture for the realisation of quantum information processing, since the two-photon interaction, or non-linearity, necessary to build logical gates can efficiently be realised by the use of interference with ancillary photons and detection [1]. Although single-photon sources and detectors are pivotal in realisations of such systems, clear guidelines for the required performance of realistic systems are yet to be defined. We present our detailed numerical simulation of several quantum optics circuits including sources and detectors all represented in multi-dimensional Fock-spaces, which allows us to obtain experimentally realistic performance bounds for these devices. In addition, the single-photon source based on switched parametric down-conversion is studied, which in principle could reach the required performance. Three approaches for implementing the switching hierarchy of the photons are simulated, and their anticipated performance is obtained. Our results define the bar for the optical devices needed to achieve the first level of linear-optics quantum computing outside the coincidence basis.

Keywords: linear optical quantum computing (LOQC); photon sources; single-photon detectors; quantum optics; quantum entanglement; numerical simulation of quantum optics

1. Introduction

With scalable linear optical quantum computing being the long term goal, even the obvious near-term experimental steps such as heralded quantum gates or creation of entangled states are very interesting applications for quantum communication, metrology and information processing. The performance of linear optical quantum computing (LOQC) relies on the quality of the various elements and devices that the system is built from, such as sources, optical elements and detectors.

The main concepts of LOQC were discovered by Knill, Milburn and Laflamme (KLM) in 2001 [1], allowing the near-deterministic performance of a scalable two-photon gate (e.g. controlled not). Within a short time, LOQC was further advanced with the discovery of one-way quantum computing [2], where the main difficulty is creating the cluster state. The original idea to create such a state is to perform KLM-type scalable gates between several photons. But later, more efficient methods for creating the cluster states have also been discovered, such as using fusion gates [3].

All these linear optical quantum computing circuits are based on the assumption of ideal elements, that is

perfect efficiency of optics, highly efficient and photon-number resolving detectors, efficiency ≈ 1 , and perfect single photon sources, output probability ≈ 1 . Even though it has recently been shown that in the asymptotic limit LOQC could work if the product of the detector efficiency and the single photon output probability is greater than $2/3$ [4], (or even greater than $1/2$ in the case of pair sources [5]), these striking results are not too practical as they require photon sources that do not emit any higher number photon numbers or multi-photon states, and very broad and complex optical circuits. A further assumption required for achieving ideal photon interference quality is that the photon wave-packets are Fourier limited and spectrally pure, and that the mode matching of the beams is ideal. Unfortunately, realistic systems will never allow us to reach the ideal case. Indeed, there are known levels of errors for performing the full scale quantum computing, which however are hard to achieve in the laboratory.

In this work we revisit the single-photon devices required for implementing basic LOQC circuits in view of achieving the next experimental level, i.e. performing the operations outside the post-selection basis.

*Corresponding author. Email: thomas.jennewein@uwaterloo.ca

Post-selection is commonly implemented in photon-experiments to cope with the inefficiencies of devices such as optical losses by only considering successful experimental runs, where the desired number of photons is actually observed. In current experimental implementations, the optical efficiencies are in the order of 10% and source efficiencies around 1%, leaving the ratio of successful to unsuccessful attempts below 10^{-6} . Therefore, current LOQC experiments involve only up to six photons, and require extensive post-selection and long measurement times. If such circuits could be performed without post-selection, quantum processing with multiple-photon would gain significant grounds and much larger numbers of photonic qubits would become accessible.

In order to understand just how well the single-photon devices must perform to reach this important goal, we studied their parameters through numerical simulation of the envisioned quantum optical circuits; we included the crucial deteriorating effects such as multi-photon emissions, optical losses and non-ideal detection. To some extent, the source and detector requirements have been addressed for measurement-based quantum computing in [3]; however, their analysis included huge numbers of sources and detectors, and some idealisations. Our simulation is experiment-driven and it aims to obtain and study accessible parameters and somewhat feasible LOQC implementations to characterise the sources and detectors.

2. Numerical simulation of quantum optics

The important feature of our approach was that every photon mode was treated as an N -dimensional Fock-space, accounting for several higher-number photon terms. Accordingly, all operators were implemented as matrices of dimension $N \times N$ obtained by matrix exponentiation of the interaction Hamiltonians, requiring significant computational resources for multi-mode optical circuits.

The numerical model was implemented in the Matlab environment, based on the quantum optics toolbox by Sze M. Tan [6]. A collection of functions and scripts were developed and specifically designed for studying single photon experiments [7]. In this model, every photon mode is represented by a Fock-space of the size N . Each state is a vector, where the first element corresponds to the amplitude of the vacuum state $|0\rangle$, and the last element corresponds to the amplitude of $N-1$ photon state, $|n-1\rangle$. It is straightforward to represent a photonic qubit, such as the polarisation of photons, as a tensor product of two such Fock-space modes. All operations on the photon

modes must be realised by an unitary evolution matrix, generated from exponentiation of the corresponding Hamiltonian. In order to explain how the representation of quantum states and operators are incorporated we have given some examples in the Appendix.

2.1. Time discretisation

This model is a monochromatic approximation of our system, therefore does not accurately incorporate any time evolution. Even though this might seem a strong approximation, it is sufficient for general simulation and analysis of LOQC type experiments. In a typical multi-photon experiment [8] the photon wave-packet is as short as 500 fs, whereas the detector electronic timing resolution is of the order of 500 ps. Hence, the detectors are essentially integrating the optical field over their timing resolution. As outlined in [9], it is possible to treat the entangling operations, such as two-photon interference, occurring between the various photons by only observing the overall behaviour of the detectable events without needing to describe and model the concrete and microscopic time evolution, as long as the generation times of the various photon are synchronised to a time better than the photon time envelopes, which is achieved by ultra-short laser pulses.

In our numerical model, we assume this condition is satisfied, and therefore the calculations are performed in a time-unit τ_d corresponding to the detector timing resolution.

2.2. Photon source

The output of the realistic photon sources are modeled with terms for single-photons ϵ , and also for the two-photons ω , as follows:

$$|\zeta\rangle = M(\sqrt{1-\epsilon^2}|0\rangle + \epsilon\sqrt{1-\omega^2}|1\rangle + \epsilon\omega|2\rangle), \quad (1)$$

with normalisation M . The single-photon performance of the source will be characterised via the second-order correlation function at zero time delay, defined as $g^{(2)}(0) = \langle a^{\dagger 2} a^2 \rangle / \langle a^{\dagger} a \rangle^2$. The output success probability of a source is the probability of finding any photons in the signal, given by the inverse of finding an empty output $P_{hrtd} = 1 - \langle 0|\zeta\rangle\langle\zeta|0\rangle$. This description of the single photon source, Equation (1), has the nice feature, that the correlation value $g^{(2)}(0)$ is essentially constant over P_{hrtd} . In particular, as this correlation value is an easily measured quality estimator it is widely used in experimental implementations of single-photon sources, and it will allow the direct relation of our simulation results to such implementations.

As one realistic implementation of photon sources we considered heralding photons from parametric down-conversion (SPDC). This will be discussed in full detail in Section 4.

2.3. Single-photon detectors

2.3.1. Bucket detector – BD

The first type is the ‘bucket detector’, which will only give a ‘click’ in the presence of photons, but will not discriminate between photon numbers. A typical example for such a detector is an avalanche photo diode (APD). The probability for a click is calculated with a projection operator, where the diagonal terms of the projector matrix take the values

$$P_{BD}(i, i) = 1 - (1 - \eta)^{(i-1)}, \quad (2)$$

where i corresponds to the particular photon number plus one, and the total efficiency η is the product of the actual detector efficiency η_{BD} with the optical efficiency η_{optics} to include losses from optical coupling and the system.

Also of interest is the operator describing an unsuccessful detection event, ‘no click’, which has the relevant applications for the suppression of higher-order terms in two-channel polarisation analysers. The corresponding projector based on the same efficiency as above, has the diagonal elements:

$$\bar{P}_{BD}(i, i) = (1 - \eta)^{(i-1)}. \quad (3)$$

These operators for successful detection and non-detection of photons are the important tools required to simulate the evolution of the quantum states and expectation values of measurements.

2.3.2. Single-photon sensitive detector – SPD

The more important type of photon detector for LOQC has the ability to discriminate photon numbers. Here we focus on the detection of one-and-only-one photon; hence named a single-photon detector (SPD). These are modelled as an operator matrix with the diagonal elements according to the probability of obtaining a positive detection signal for a given input photon state, which for a given total efficiency η has the following diagonal terms:

$$P_{SPD}(i, i) = (i - 1)\eta(1 - \eta)^{(i-2)}, \quad (4)$$

as well as the the No-Click-projector

$$\bar{P}_{SPD}(i, i) = (1 - \eta)^{(i-1)}, \quad (5)$$

where as above, the efficiency is $\eta = \eta_{SPD} * \eta_{optics}$, the product of the intrinsic detector efficiency and the optical system, and i ranges from $1, \dots, N$.

2.3.3. Noise and saturation of the photon detectors

In addition to the main deficiency of detectors, which is the limited efficiency, they also show error detections due to dark counts. This describes the behaviour of detectors to give false detection events, even if no signal is present. We model this by adding a constant term ϵ_d , corresponding to the probability of a noise-induced detection signal per time unit τ_d , to each element of the detector’s operator:

$$P_{ndet}(i, i) = P(i, i)_{BD/SPD} + \epsilon_d. \quad (6)$$

Generally, one must take care that the final calculated probability for a detection will in general not be continuous, but rather must also include a maximal cutoff at unity, which actually corresponds to saturation of the detector. The probability for a detection event would then be limited to unity in the following relation $P = \max(\text{Tr}(P_{ndet}|\Phi), 1)$. It is straightforward to see why this should be correct: in the case of a unit efficiency detector with a dark count probability ϵ_d , the final detection probability of a signal will be offset by this amount, until the level of unity is reached and the detector saturates. However, in all practical cases that are considered here, the detection probability per time-unit is significantly less than unity, and therefore this cutoff must not be implemented.

In the case of the No-Click projector we subtract ϵ_d from each term; however, it must be ascertained that none of the values becomes negative. More practically in actual experiments, the dark count rate can be efficiently decreased by an appropriate time gating, triggered, for instance, by the main pump laser.

3. Simulation of LOQC circuits and the results

With the numeric modelling of quantum optics in place we were able to conduct a series of simulations on interesting linear optical quantum circuits. The chosen small selection is representative for both the existing experiments – non-scalable gates that operate in post-selection – as well as for the next steps towards future implementations of LOQC – scalable gates, that do not require post-selection. What is unique in our approach is that we aimed to follow the practical experimental implementation for the studied quantum circuit, as well as the actual methods for generating single photons from cascaded down-conversion and non-perfect single-photon detectors.

3.1. C-Phase gate – non-scalable scheme 1

We simulate the creation of Bell-pairs of photons (see Figure 1(a)) which is easily achieved by making two photons interfere on a partial polarising beam-splitter (PPBS), which acts as a controlled-phase (c-phase) gate [10]. This is non-scalable operation, as it can only work in post-selection meaning that the desired photon state is extracted by detection of the photons. This scheme can, in general, not be concatenated to implement more complex operations, except in few very special cases as illustrated in the next section. The quality of the output is assessed via the violation of the Bell-pair witness [11], as well as the Clauser-Horne-Shimony-Holt-inequality (CHSH-inequality) violation [12].

We find from the simulation that in this case the involved single photon sources must show a $g^2(0)$ -correlation less than 0.15 in order that a Bell-inequality can be violated, and less than 0.39 in order to satisfy the Bell-state witness [13]. Due to post-selection, the actual detection efficiency and the success probability of the setup are not fundamental issues as they only affect the achievable count rate but not the quality of the output.

3.2. Two C-Phase gates – non-scalable scheme 2

By chaining two of the above-mentioned non-scalable c-phase gates (Figure 1(b)), it is possible to entangle

three photons into a Greenberger-Horne-Zeilinger-state (GHZ). As was the case of just one c-phase gate, this circuit can only work in post-selection and is therefore not scalable. We reconstruct the value of the witness for a GHZ state [13] from our simulation as the quantitative criterion to assess the performance of the entangling operation.

Our simulation shows that the required quality of the single-photons must be to provide an output with a $g^2(0)$ correlation less than 0.06, which is already a huge challenge to achieve. Also in this case, the efficiency of the detectors and of the source only affects the count rate.

3.3. KLM-type gates – scalable scheme 1

In order to achieve bounds for the next important step towards LOQC, we simulated the heralding of Bell-pairs with KLM-type gates. Thereby, the control and target photons interact via the assistance (effectively two-photon interferences) of two ancillary photons. The final detection of the ancillary photons flags a successful run of the gate, and the control and target photon are retrievable – and reusable – from their outputs. These gates are fully scalable and can build arbitrary circuits. It is important to note that these gates require single-photon resolving detectors.

We focused our simulation in particular on the simplified KLM-gate [14] (Figure 2(a)). We also studied the cases of the Knill-gate [15] and the

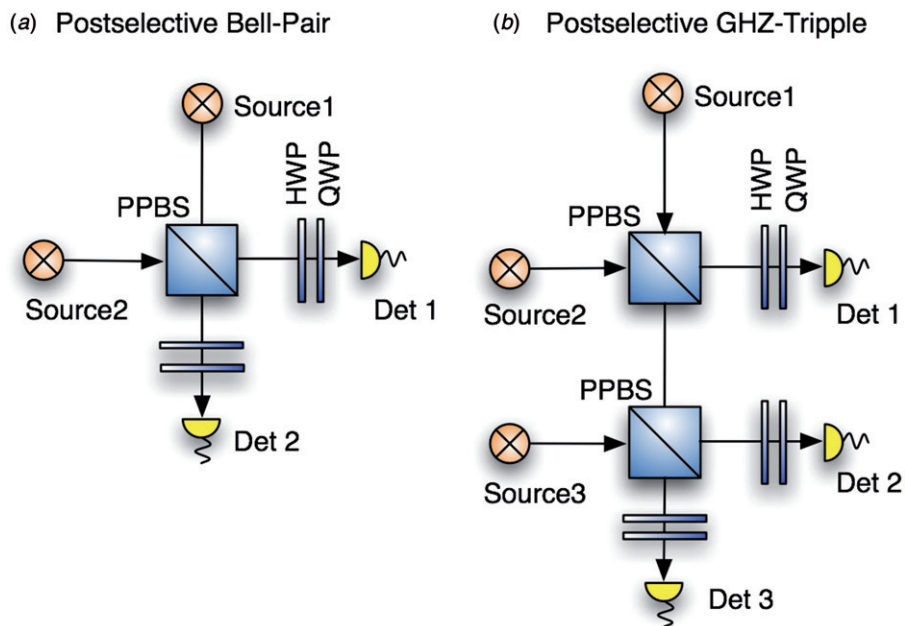


Figure 1. Schematics of the two post-selective (and therefore non-scalable) quantum circuits that were studied here. (a) Post-selective implementation of a c-phase gate, used to create a Bell-pair of photons; (b) scheme of concatenated c-phase gates for creating Greenberger-Horne-Zeilinger (GHZ)-triples of photons. (The colour version of this figure is included in the online version of the journal.)

Pittman-Franson-gate [16]. We observed that the former has performances nearly identical to the KLM gate. Concerning the latter, this is harder to implement, as it requires a Bell pair as an ancilla; this demands either a deterministic entanglement source or a KLM gate on its own.

In order to test the operation of the gate we chose to follow exactly what a possible experimental situation would be in order to prove that this gate was successfully realised: we observed the pair-wise correlations of the output photons for the Clauser-Horne (CH) inequality [17], which explicitly excludes post-selection in the measurements or analysis. In addition, we also studied the witness for a Bell-state.

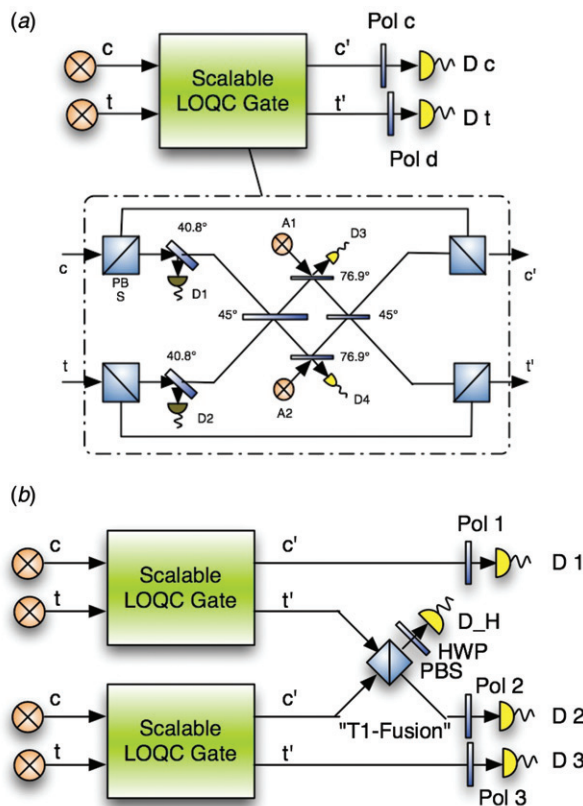


Figure 2. Schematics of the simulated scalable-LOQC circuits. (a) Scalable linear optical gate called the simplified-KLM-gate (inset), utilised to create heralded Bell-pairs of photons from the initially separable input photons. The successful operation of this gate is flagged by the detection of the two ancillary single photons in their outputs. The quality of the gate is observed by testing the CH-Bell-inequality on the entangled photons, which does not allow for any post-selection on the output states. (b) As the first level of the one-way quantum computing with cluster states the direct and heralded generating of a three-photon GHZ state is studied. GHZ-states are created from two heralded Bell-pairs generated in the simplified-KLM-gate, connected via a type-I Fusion gate. (The colour version of this figure is included in the online version of the journal.)

A good way of presenting the photon-source requirements is to plot of their performance in terms of $g^{(2)}(0)$ -correlation as well as the success probability for heralding a single photon (see Figure 3) 1-KLM plots. Summarising all the simulation results becomes very cumbersome, as many parameters in the simulation are varied, and extracting the actual interesting information is hard for the reader. Here, as can be seen in the figure, the total system efficiency (i.e. optics+detectors) becomes crucial. Only at the total system efficiency above $\eta=0.9$ and single-photon resolving detection does the simplified-KLM-gate perform in a useful manner. In this case, to give concrete numbers, if the probability for the source to herald single photons is 0.8 then the required $g^{(2)}(0)$ -correlation must be below 0.03 in order to violate the CH-inequality. Notably, satisfying the Bell-state witness can only be achieved if the probability for the source to herald single photons is above 0.9, then the $g^{(2)}(0)$ -correlation may become as high as 0.045. The source requirements do become relaxed if the system-detection efficiency is higher than 0.9.

3.4. One-way quantum computing – scalable scheme 2

Cluster-state quantum computing can be efficiently realised if a source of heralded GHZ-entangled photons is available. There are many approaches to directly creating such states, however, LOQC itself offers the possibility to generate a heralded GHZ state by fusing two Bell-pairs created from separate KLM-gates, as outlined in [3] (Figure 2(b)). The fusion-operation is in the interference of two-photons on a beam-splitter and detection of exactly one photon in one output arm. The resulting GHZ-entangled state of the three photons is tested against a Mermin-type inequality [18] and a GHZ-state witness [13].

The simulation of this scenario became very resource-hungry, since the total amount of modes is rather large. The main outcomes from the simulations clearly show that this scenario will also be very challenging to realise. The total detection efficiency η should be at least 0.95, and the requirements for the photon-sources are tight, asking for a probability for heralding output photons $P_{herld} > 0.97$ and the $g^{(2)}(0)$ -correlation of 0.01. Reaching such requirements will be very challenging for any optical systems.

4. Generating single photons

These simulations have provided the baseline for the requirements that such LOQC circuits pose on photon-sources and photon-detectors. In the following

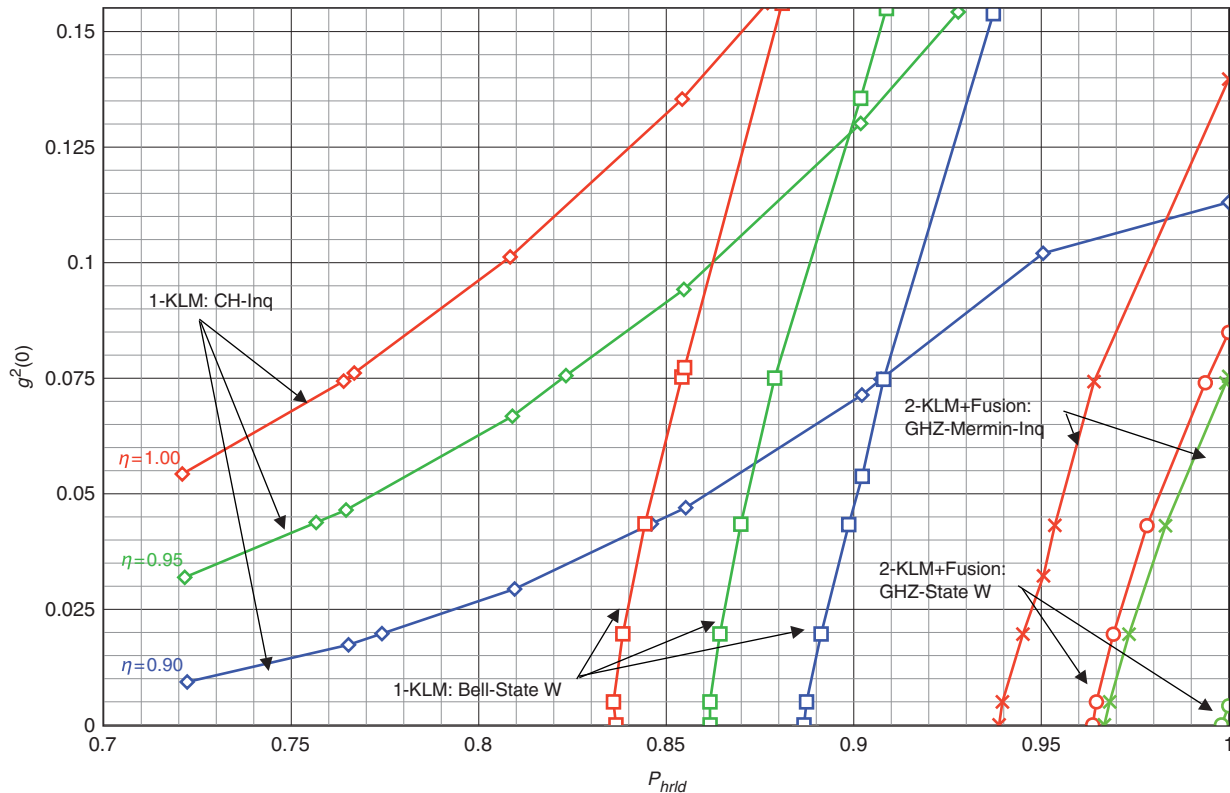


Figure 3. Numerical results of source and detector performance required to achieve performing simple LOQC circuits without post-selection. 1-KLM denotes the calculation where two photons are entangled into a Bell-state via one simplified Knill-Laflamme-Milburn gate; 2-KLM denotes the operation where two such Bell-states are fused, and a 3-photon GHZ state is created. The vertical axis is the second-order correlation of the photon source beams, $g^2(0)$ at zero time delay. The horizontal axis is the probability that the involved photon sources do fire upon a trigger and herald a photon signal, P_{hrld} . The simulations were performed assuming total efficiencies (optical and detectors) between $\eta=0.90$, 0.95 , 1.00 , coded in blue, green and black. The simulation showed that the total efficiency must be greater than about $\eta=0.9$ to deliver useful results in the 1-KLM case, and above $\eta=0.95$ for the 2-KLM case. (The colour version of this figure is included in the online version of the journal.)

it will be studied, if, and how, a single-photon source based on parametric down-conversion might be able to reach these challenging parameters.

The present most important source for multiple and entangled photons is spontaneous parametric down conversion [19], which is essentially the spontaneous emission from an optical parametric amplifier, also referred to as a squeezed vacuum. When observing the two output modes of the squeezer, photons are produced in pairs, and therefore the correlations are sub-Poissonian, and therefore enable conditional single-photon experiments. However, given the non-deterministic behaviour of this interaction, the photon-state created from SPDC produces not only single photon-pair terms, but also multiple numbers of photon-pairs.

4.1. Modelling of SPDC

The Hamiltonian that describes the interaction in SPDC is the simplified squeezing operator, which has

the approximation of a strong pump mode, and acts on two output modes a_1, a_2 in the form

$$H_{SPDC} = \epsilon(a_1^\dagger a_2^\dagger + a_1 a_2), \quad (7)$$

where ϵ is the squeezing parameter. The evolution of this Hamiltonian is calculated via matrix exponentiation. Obviously, our numerical model takes account of all higher order photon number terms with their full and correct amplitude, which can then easily be propagated through any quantum circuits simulation, such as logic gates.

4.2. Heralding photons from SPDC

Based on the SPDC state produced from squeezing, we want to study in detail the quality of heralded single photon states achieved by detecting one mode from the SPDC source, and correspondingly heralding a single photon in the other. Given the strict photon pair correlations imposed by the squeezing operator, this could deliver perfect single photons, if it would

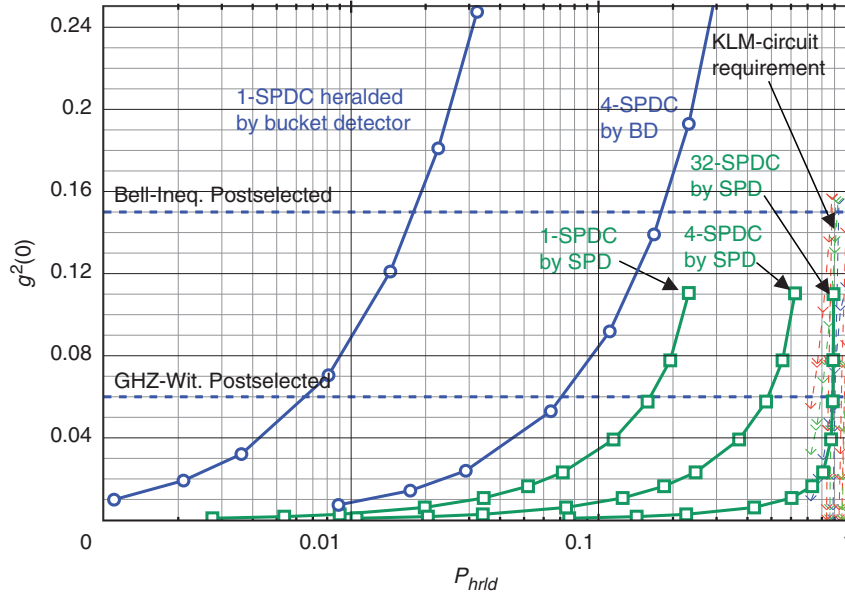


Figure 4. Combination of the results from the numerical simulations of the LOQC with the single photon source from SPDC. The many superimposed plots in the right corner show the area of interest that is required to be reached by a good single-photon source. The data named *1-SPDC* corresponds to a photon source based on heralded photons created from spontaneous parametric down-conversion, heralded with either a bucket detector (BD) with efficiency $\eta = 0.8$ or a single photon detector (SPD) with $\eta = 0.95$. The switch for the SPDC photons is a binary switch, assuming each level has a transmittance of 0.98, and in addition, the coupling efficiency of the entangled photons is 0.98 each. The curve labelled *n-SPDC* shows the performance for photons generated from the switching of multiple SPDC sources. The parameter of the source curves is the squeezing parameter of the SPDC process. The faint plots on the lower right corner are the requirement data for achieving KLM-type operations outside the coincidence basis (see Figure 3). In addition, the graph contains the thresholds for post-selective circuits such as creating a Bell-pair or a GHZ-triplet. In these cases the probability of the source, P_{hrld} to generate a photon signal has no effect on the threshold. It is obvious, that photon sources based on heralding from one SPDC (1-SPDC) will never reach the areas of performance required for post-selection free LOQC operations. (The colour version of this figure is included in the online version of the journal.)

not be for the higher order emissions. Various combinations and parameters of the heralded photons are modelled, and the produced state is analysed. Since the detection process on the trigger photon corresponds, at least in principle, to a photon number measurement, the remaining photon is no longer in a superposition of number states, as originally given by the SPDC. Now it is actually a density matrix, which is represented as an array of number states weighted with amplitudes corresponding to the correct probability. In Figure 6 (1-SPDC), the variation of $g^{(2)}(0)$ correlation versus the probability for heralding a photon are shown as the important characteristics of the created photon state, in dependence of the squeezing parameter ϵ for one SPDC source.

The output state from SPDC is generated from acting the operator on vacuum, $U_{SPDC}|0, 0\rangle_{a_1, a_2}$, which yields:

$$|SPDC\rangle = C_0|00\rangle_{a_1, a_2} + C_1|11\rangle_{a_1, a_2} + C_2|22\rangle_{a_1, a_2} + \dots \quad (8)$$

the detection on the photon of side a_1 with a photon detector gives us the conditional output state on

side a_2 , leading to a mixture of photon number states, which can potentially be closer to an ideal single photon:

$$\rho_{heralded1} = \text{Tr}_{a_1}(P_{BD a_1}|SPDC\rangle) \quad (9)$$

$$= \left\{ Q|0\rangle\langle 0|_{a_2}; P_1|C_1|^2|1\rangle\langle 1|_{a_2}; P_2|C_2|^2|2\rangle\langle 2|_{a_2}; \dots \right\} \quad (10)$$

where P_1, P_2, \dots are the detection probabilities for a ‘click’, as defined in expression 2, the C_1, C_2, \dots are the amplitudes of the terms from the SPDC state, and $Q = 1 - \sum P_i|C_i|^2$, is the probability of not finding a trigger detection event in mode a_1 , or the vacuum term. The quality of one such heralded single photon state is measured as the $g^{(2)}$ -correlation function [20], versus the probability for obtaining a successful heralding event. It is evident that heralded photons from SPDC are far from being useful for LOQC, as they are far from the required performance. In particular, the strength of the SPDC must be kept sufficient low such that the detection probability of the trigger is

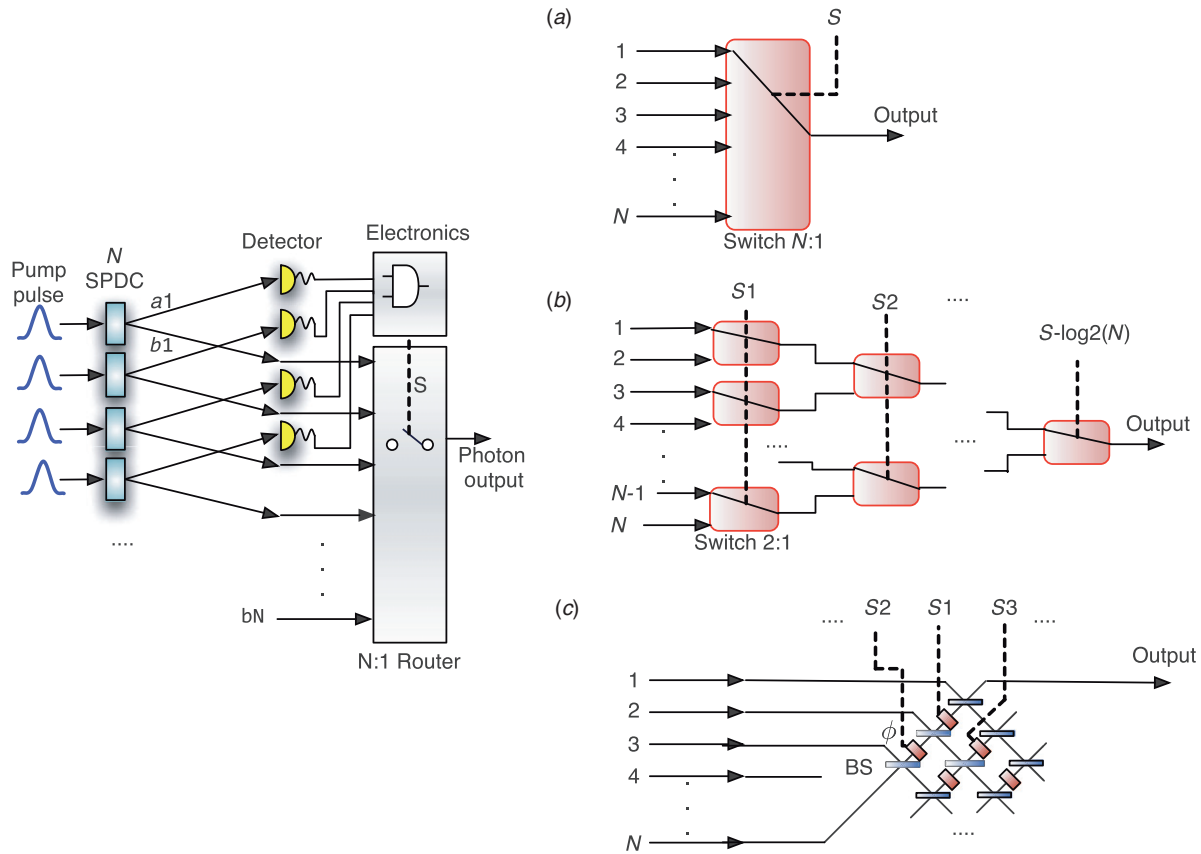


Figure 5. (Left) Heralding single photons from N spontaneous parametric down conversions (SPDC), each pumped by tightly synchronized ultra short pump pulses. Depending on the trigger detection modes a_1, \dots, a_n , the corresponding routing signals from modes b_1, \dots, b_N are switched to the output. (Right) Depicted are three main architectures for implementing the routing switch. (a) One linear mode-switch, (b) binary coded mode-switches, (c) interferometric multi-port with phase modulators. The number of optical components in each photon path depends on the variant and therefore the loss will have fundamentally different scaling with the number of input modes N . (The colour version of this figure is included in the online version of the journal.)

below 0.1 in order maintain a single photon purity of better than 90% (see the 1-SPDC plots in Figure 6). If the squeezing parameter, ϵ becomes to large, then the single-photon quality is drastically deteriorated.

The best approach in improving the output quality from from SPDC is to ‘chain’ several such sources with active switches [21,22], see Figure 4. Thereby, several probabilistic sources are effectively combined into one deterministic source, which in principle can be made arbitrarily close to the ideal case. It is straightforward to study the characteristics of this switched SPDC source into the model, by keeping the squeezing parameter ϵ fixed at a certain value, and varying the number S of SPDC sources that are combined. The heralded state is obtained from the original heralded single photon state, and yields

$$\rho_{\text{heralded}S} = \left\{ Q^S |0\rangle\langle 0|_{a2}; \frac{(1-Q^S)}{(1-Q)} P_1 |C_1|^2 |1\rangle\langle 1|_{a2}; \frac{(1-Q^S)}{(1-Q)} P_2 |C_2|^2 |2\rangle\langle 2|_{a2}; \dots \right\}. \quad (11)$$

From the analysis shown in Figure 6 it is clear that this type of heralding source outperforms a standard SPDC scheme, even at modest squeezing parameters and number of sources equal to four. In fact, this type of source may constitute a viable single photon source, given that other quantum systems such as quantum dots [23,24] or single stored ions [25] face the challenge of achieving good coupling efficiencies.

4.3. Considering losses in the switches

In any practical implementation of the SPDC-switch schemes the total losses will scale with the amount of input modes that should be accommodated. The schemes shown in Figure 4 each have their advantages and disadvantages, however, it is crucial that they allow a scalable operation at all. Scheme A is the most efficient, as each photon only passes through one switch before entering the output mode. Therefore, the overall system losses are constant, and do not change with the number of sources. Scheme B is also very

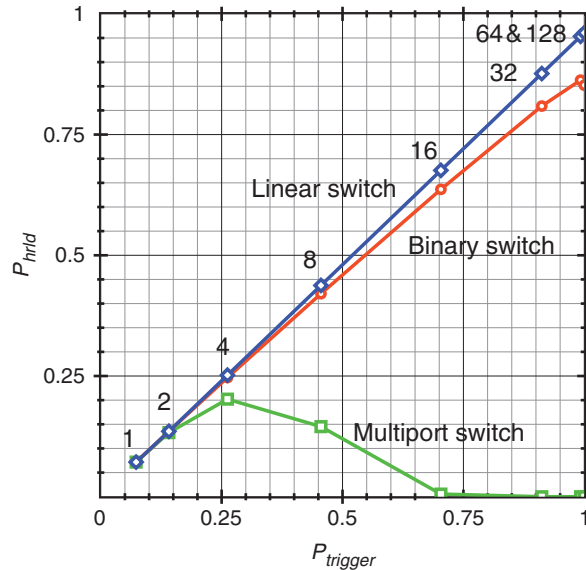


Figure 6. Photon heralding efficiency versus the probability for a trigger, P_{trigger} , for different numbers of sources (1, 2, 4, ..., 128), as given as parameter on the plots. P_{hrd} is the probability of obtaining a non-zero photon output of the source. Three types of switches are considered, as discussed in the text, and the switching efficiency is assumed to be 0.98 per element. (The colour version of this figure is included in the online version of the journal.)

efficient, and consists of a cascade of binary switches. The amount of elements each photon must pass through is on scales with the logarithm of the number of sources, $\log_2(N)$. Finally, scheme C is a multi-input interferometer, with N inputs and 1 output, where the inputs are routed interferometrically to the output, e.g. via active phase changes. The interferometer follows the generalised rules for multi-ports [26], where, of the order of N^2 optical elements, including beam-splitters and phase shifters, can realise any unitary operation.

From our simulation we obtained the probability for heralding a single-photon output versus trigger probability, for an increasing number of SPDC sources, see Figure 5. These results clearly show that a linear (scheme A) or binary (scheme B) arrangement of switches can be useful for generating single-photon states sufficient for LOQC, whereas the multipoint type (scheme C) of switch will fail due to the scaling of losses with additional switching layers.

5. Conclusions

We described a numerical simulation of the quantum optics of LOQC, specifically tailored to obtain the characteristics of single-photon sources and photon

detectors required to perform quantum computing operations in actual experiments.

First, we studied the heralding of Bell-pairs with scalable KLM-gates [1] where two photons, the control and target, are entangled via the assistance and detection of two ancillary photons. These gates are fully scalable and could be combined into arbitrary quantum logic. The operation was verified by testing the correlations of the output photons against the CH inequality [17], without post-selection.

Secondly, we simulated the creation of heralded Greenberger-Horne-Zeilinger (GHZ) states via fusing [4] two Bell-pairs created with separate KLM-gates as the first building block of a cluster-state quantum computer [2]. The resulting GHZ state was tested via a Mermin-type inequality [18] and a GHZ-state witness [10], all without post-selection.

Our results show that performing LOQC operations outside the post-selection basis requires photon-detectors with efficiencies of about 0.90, single-photon sources with a success probabilities close to 0.90 and single-photon purities ($g^{(2)}$ -correlation function) better than 0.07, as a guideline. These performance levels will be challenging to reach in real systems, but not impossible in our view. We compare these requirements with performance of state-of-the-art single photon sources based on down-conversion and cascaded down-conversion, as well other implementations. Our study is the first to establish precise guidelines for developing single-photon devices in respect of the implementing optical quantum processing applications.

Acknowledgements

We are grateful for useful discussions with T. Ralph, G. Milburn and T. Rudolph. T.J. and A.G.W. acknowledge support by the Australian Research Council (Linkage and Federal Fellowship). M.B. acknowledges support by the Marie Curie action of the EU Commission, PIEF-GA-2009-236345-PROMETEO.

References

- [1] Knill, E.; Laflamme, R.; Milburn, G.J. *Nature* **2001**, *409*, 46–52.
- [2] Raussendorf, R.; Briegel, H.J. *Phys. Rev. Lett.* **2001**, *86*, 5188–5191.
- [3] Browne, D.E.; Rudolph, T. *Phys. Rev. Lett.* **2005**, *95*, 010501.
- [4] Varnava, M.; Browne, D.E.; Rudolph, T. *Phys. Rev. Lett.* **2008**, *100*, 060502.
- [5] Gong, Y.-X.; Zou, X.-B.; Ralph, T.C.; Zhu, S.-N.; Guo, G.-C. *Phys. Rev. A* **2010**, *81*, 052303.

- [6] Tan, S.M. *J. Opt. B: Quantum Semiclassical Opt.* **1999**, *1*, 424–432.
- [7] Jennewein, T. Toolbox for Quantum Photonics in Matlab. <http://info.iqc.ca/qpl/> (accessed June 1, 2010).
- [8] Bouwmeester, D.; Pan, J.W.; Mattle, K.; Eibl, M.; Weinfurter, H.; Zeilinger, A. *Nature* **1997**, *390*, 575–579.
- [9] Zukowski, M.; Zeilinger, A.; Weinfurter, H. *Ann. N.Y. Acad. Sci.* **1995**, *755*, 91–102.
- [10] Langford, N.K.; Weinhold, T.J.; Prevedel, R.; Resch, K.J.; Gilchrist, A.; O'Brien, J.L.; Pryde, G.J.; White, A.G. *Phys. Rev. Lett.* **2005**, *95*, 210504.
- [11] Barbieri, M.; De Martini, F.; Di Nepi, G.; Mataloni, P.; D'Ariano, G.M.; C. Macchiavello. *Phys. Rev. Lett.* **2003**, *91*, 227901.
- [12] Clauser, J.F.; Horne, M.A.; Shimony, A.; Holt, R.A. *Phys. Rev. Lett.* **1969**, *23*, 880–884.
- [13] Gühne, O.; Hyllus, P. *Int. J. Theoret. Phys.* **2003**, *42*, 1001–1013.
- [14] Dodd, J.L.; Ralph, T.C.; Milburn, G.J. *Phys. Rev. A* **2003**, *68*, 042328.
- [15] Knill, E. *Phys. Rev. A* **2002**, *66*, 052306.
- [16] Pittman, T.B.; Jacobs, B.C.; Franson, J.D. *Phys. Rev. A* **2001**, *64*, 062311.
- [17] Clauser, J.F.; Horne, M.A. *Phys. Rev. D* **1974**, *10*, 526–535.
- [18] Mermin, N.D. *Phys. Rev. Lett.* **1990**, *65*, 1838–1840.
- [19] Klyshko, D.N. *JETP Lett.* **1967**, *6*, 23.
- [20] Mandel, L.; Wolf, E. *Optical Coherence and Quantum Optics*; Cambridge University Press: Cambridge, 1995.
- [21] Kumar, P.; Kwiat, P.; Migdall, A.; Nam, S.W.; Vuckovic, J.; Wong, F.N.C. *Quantum Inf. Process.* **2004**, *3*, 215–231.
- [22] Ma, X.-S.; Zotter, S.; Kofler, J.; Jennewein, T.; Zeilinger, A. *Towards on-demand Single-photon Generation via Active Multiplexing*. 2010, arXiv: 1007.4798v1 e-Print archive. http://arxiv.org/PS_cache/arxiv/pdf/1007/1007.4798v1.pdf.
- [23] Badolato, A.; Hennessy, K.; Atature, M.; Dreiser, J.; Hu, E.; Petroff, P.M.; Imamoglu, A. *Science* **2005**, *308*, 1158–1161.
- [24] Michler, P.; Kiraz, A.; Becher, C.; Schoenfeld, W.V.; Petroff, P.M.; Zhang, L.; Hu, E.; Imamoglu, A. *Science* **2000**, *290*, 2282–2285.
- [25] Barros, H.G.; Stute, A.; Northup, T.E.; Russo, C.; Schmidt, P.O.; Blatt, R. *New J. Phys.* **2009**, *11*, 103004.
- [26] Reck, M.; Zeilinger, A.; Bernstein, H.J.; Bertani, P. *Phys. Rev. Lett.* **1994**, *73*, 58–61.

Appendix

Examples of states and operators represented in the numerical model

Quantum states are modelled as vectors, where each element is considered as the amplitude of this particular excitation. Therefore, all elements of the vectors and operators must obey the normalisation rules.

For example (for the dimension of the Fockspace $N=4$), the vacuum state is a vector with amplitude on the first

element

```
>> vacc
vacc=Quantum object
Hilbert space dimensions [4] by [1]
    1
    0
    0
    0
```

Consequently, a single photon state is represented as the following vector:

```
oneph=Quantum object
Hilbert space dimensions [5] by [1]
    0
    1
    0
    0
    0
```

And the state that describes a superposition of vacuum and one photon has the form:

```
>> 1/sqrt(2)*(vacc+oneph)
ans=Quantum object
Hilbert space dimensions [4] by [1]
    0.70711
    0.70711
    0
    0
```

In this model, any operator acting on a single mode (such as the creation or annihilation operators, phase shifter) are represented as $N*N$ matrices. Consequently, interaction Hamiltonians are expressed in the form of creation and annihilation operator matrices (example with $N=4$):

```
a=Quantum object
Hilbert space dimensions [4] by [4]
    0    1    0    0
    0    0    1.4142    0
    0    0    0    1.7321
    0    0    0    0
```

```
>> a'
ans = Quantum object
Hilbert space dimensions [4] by [4]
    0    0    0    0
    1    0    0    0
    0    1.4142    0    0
    0    0    1.7321    0
```

and the unitary evolution is obtained through exponentiation $U_{bs} = \exp(-i*H_{bs})$.

The extension of a higher number of modes is realised by attaching the two (or more) modes through the tensor product:

```
>> tensor(oneph,vacc)
ans=Quantum object
Hilbert space dimensions [5 5] by [1 1]
    (6,1)    1
```

As an example, the operator representing a 50:50 beam-splitter, which is a two-mode operator, is a N^2*N^2 matrix. It is based on the two-mode Hamiltonian

$$H_{bs} = \theta(a_1^\dagger a_2 + a_1 a_2^\dagger). \quad (12)$$

As an example, this looks as follows:

```
%Beam splitter 50:50=Quarter wave plate @45
eta=1*pi/4;
H_bs=(tensor(a,a')+tensor(a',a))*eta;
U_bs=expm(-1i*H_bs);

>> U_bs
U_bs=Quantum object
Hilbert space dimensions [5 5] by [5 5]
(1,1)      1
(2,2)      0.70711
(6,2)      0 -      0.70711i
(3,3)      0.5
(7,3)      0 -      0.70711i
(11,3)     -0.5
(4,4)      0.35355
(8,4)      0 -      0.61237i
(12,4)     -0.61237
(16,4)     0 +      0.35355i
(5,5)      0.25
(9,5)      0 -      0.5i
.....
```

Density matrices are also represented as matrices, and also can be subject to tensor-products, evolution with operators as well as detections. For example, the single photon state will have a density operator of the form:

```
>> oneph*oneph'
ans=Quantum object
Hilbert space dimensions [4] by [4]
 0 0 0 0
 0 1 0 0
 0 0 0 0
 0 0 0 0.
```

And as for the example of the equal superposition of the vacuum state and one photon, the density matrix takes the form:

```
>> sup=1/sqrt(2)*(vacc+oneph);
>> sup*sup'
ans=Quantum object
Hilbert space dimensions [4] by [4]
 0.5 0.5 0 0
 0.5 0.5 0 0
 0 0 0 0
 0 0 0 0.
```

This can also be represented in the form of Ket and Bra,

```
>> display_state4(N,sup)

ans=

'Purestate=
0.707*'
'|0,> 1.000 '
'|1,> 1.000 '
```

Single-photon detectors

We give examples of the concrete representation of single photon detectors. The operator for a Bucket-detector, with efficiency of 0.6, a noise factor of 0.001

has the form:

```
>> [bdbl_n]=BucketDetector_noise(N,0.6,0.001)
bd=Quantum object
Hilbert space dimensions [4] by [4]
 0.001 0 0 0
 0 0.601 0 0
 0 0 0.841 0
 0 0 0 0.937

bd_n=Quantum object
Hilbert space dimensions [4] by [4]
 0.999 0 0 0
 0 0.399 0 0
 0 0 0.159 0
 0 0 0 0.063
```

where bd is used to calculate the probability for obtaining a detection event, and bd_n the probability for not obtaining a detection. The actual probabilities for the detection of a photon are obtained by taking the expectation value of the detector matrix with the respected quantum state.

For our example with the previously defined operators bd and bd_n , the actual probabilities for observing a Click or a Non-Click for a one-photon state, $oneph$, are easily computed as expectation values:

```
>> (oneph'*bd*oneph)
ans=Quantum object
Hilbert space dimensions [1] by [1]
 0.601

>> (oneph'*bd_n*oneph)
ans=Quantum object
Hilbert space dimensions [1] by [1]
 0.399.
```

Modelling spontaneous parametric down-conversion

The evolution of the Hamiltonian in equation 7 which describes SPDC, can be calculated via matrix exponentiation, $U_{SPDC} = \expm(-iH)$, which for example takes the form ($N=4$, $\epsilon=0.4$):

```
%SPDC in chi2:
H_chi2=(tensor(a,a)+tensor(a',a'))*epsilon;
U_chi2=expm(-1i*H_chi2);
```

```
%SPDC input state for pair of photons in HH
spdc_state=U_chi2*tensor(vacc,vacc);
```

```
U_chi2=Quantum object
Hilbert space dimensions [4 4] by [4 4]
(1,1)      0.925
(6,1)      0 -      0.35162i
(11,1)     -0.13218
(16,1)     0 +      0.057186i
(2,2)      0.85635
(7,2)      0 -      0.4525i
(12,2)     -0.2488
(3,3)      0.76945

(8,3)      0 -      0.63871i
(4,4)      1
...
```

It is straightforward to calculate the state produced by the SPDC operator, by multiplying this operator matrix with a given input state, in this case a vacuum (i.e. $|0\rangle = [1, 0, 0, 0]$), $|SPDC\rangle = U_{SPDC} * \text{tensor}([1, 0, 0, 0], [1, 0, 0, 0])$, giving the output state of the down-converter:

```
spdc_state=Quantum object
Hilbert space dimensions [4 4] by [1 1]
(1,1)          0.925
(6,1)          0 - 0.35162i
(11,1)         -0.13218
(16,1)         0 + 0.057186i
```

where the (1,1) term corresponds to $|00\rangle_{a_1, a_2}$ output, the (6,1) term corresponds to $|11\rangle_{a_1, a_2}$, (11,1) corresponds to $|22\rangle_{a_1, a_2}$

and so on. Expressed with Kets representing the photon number, the SPDC state has the following form:

```
>> display_state4(N,spdc_state)

ans=

'Pure state=
0.925 * '
'|0,0,> 1.000 '
'|1,1,> 0.000-0.380i '
'|2,2,> -0.143 '
'|3,3,> 0.000+0.062i ' .
```